Received: 13 May 2019 | Revised: 5 February 2020 | Accepted: 14 February 2020

DOI: 10.1002/pep2.24155

PeptideScience WILEY

FULL PAPER

Interactions of rationally designed small peptide dendrons functionalized with valine or sinapic acid with α-helix and β-sheet structures of poly-L-lysine and poly-L-glutamic acid

Maja Morawiak[1] | Magdalena Stolarska[2] | Maciej Cieślak[1] | Zofia Urbanczyk-Lipkowska[1]

[1]Institute of Organic Chemistry Polish Academy of Sciences, Warsaw, Poland

[2]Department of Chemistry, Gdansk Polytechnic School, Gdańsk, Poland

Correspondence
Zofia Urbanczyk-Lipkowska, Institute of Organic Chemistry Polish Academy of Sciences, Warsaw, Poland.
Email: zofia.lipkowska@icho.edu.pl

Funding information
National Science Centre of Poland, Grant/Award Number: UMO-2012/07/B/ST5/01941

Abstract

Uncontrolled protein oligomerization leading to deposition of fibrils is related to several diseases including neurodegeneration and diabetes. Involvement of natural compounds in regulation of this process has been documented. Therefore, the design and detailed study of bioinspired new molecular entities is one of the possible avenues to achieve better therapeutics. Here, we provide experimental data derived from the application of chiraloptic methods that rationally designed, bioinspired small branched peptides influenced the primary conformation of both poly-L-lysine (PLL) and poly-L-glutamic acid (PLGA) polypeptides in a structure- and concentration-dependent manner. In several cases, the circular dichroism (CD) spectra of polypeptide/dendron mixtures were considerably different from those corresponding to the individual polypeptides, in terms of significant reduction of intensity, discrete structure, and dislocation of characteristic bands. Data deconvolution suggested that compared to the individual homo-polypeptides, the resulting polypeptide/dendron complexes had a relative gain of distorted α-helix, and right- and left-hand twisted β-sheet forms, which may indicate a more diffuse structure. The electrostatic attraction and multiple hydrogen bonding between oppositely charged molecules, that is, between cationic-branched peptides and the β-sheet surface formed by anionic PLGA, might be the main cause of coaggregation that increased the variety and contribution of less ordered forms, and reduced the propensity for self-aggregation.

KEYWORDS

branched peptides, circular dichroism, fibrillation, sinapic acid, supramolecular interactions, valine

1 | INTRODUCTION

Protein folding and aggregation are natural cellular processes coded by the amino acid sequence. Folding enables construction of well-defined 3D structures that are specific for a particular protein. The resulting structure is characterized by a multifunctional surface that is critical for various protein functions, such as molecular recognition, transport, specificity of ligand binding, and further transformations. Moreover, as documented by numerous X-ray studies of proteins or enzymes, formation of an active site is often assigned not to a monomer unit but to protein aggregates. In homeostasis, proteins in monomeric and aggregated form are recognized, disassembled, cleaved, and recirculated by the cell's enzymatic machinery (*e.g.*, chaperones, enzymes, etc.).[1,2] In pathological conditions misfolded proteins may be involved in a process of self-assembly that cannot be controlled, leading to formation of fibrillary deposits that are problematic for cell

function and survival. Oligomerization of misfolded proteins under impaired functioning of the chaperone protection system is thought to be associated with a number of human diseases, including Alzheimer's disease, Parkinson's disease, and diabetes.[3]

Therefore, molecules that suppress self-aggregation or eliminate abnormal and/or toxic protein aggregates are in high demand. Recently two types of compounds have demonstrated their usefulness in controlling the aggregation process: small amphiphilic peptides and natural polyphenols that are part of the molecular recognition machinery and are regarded as defense against unwanted pro-oxidation processes. The peptide-based design strategy was based on the knowledge of strategic fragments in the amyloid beta peptide (Aβ) sequence that, due to supramolecular interactions (electrostatic, hydrophobic-hydrophobic or hydrogen bonding), are responsible for Aβ self-recognition and further oligomerisation.[4] A great example is the (Aβ17-21) sequence 5-peptide (Leu-Val-Phe-Phe-Ala) that has been modified on the N- or C-terminus by coupling with basic amino acid(s) or PEG fragments to obtain well-soluble 7 to 15 amino acid long peptides that disturb fibril formation and promote disassembly of the preformed fibrils.[5] As revealed in a recent study in an animal model of Alzheimer disease, even more spectacular is the discovery of the anti-aggregative potential of sinapic acid, a natural polyphenol with a cinnamic acid structure.[6] It was found in two independent *in vivo* studies that cognitive impairment associated with Alzheimer disease, induced by injection of amyloid β (Aβ) 1-42 protein in mice[7] or scopolamine in rats,[8] was abolished after oral administration of sinapic acid.

A fundamental principle of the normal or pathogenic fibrillation process is the primary intermolecular recognition between protein fragments of complementary chemical character. This idea was recently used to explore chromatographic beads enriched with single amino acids to form bulky hexapeptide combinatorial libraries for capturing low abundant proteins from a mixture of natural origin.[9] It appeared that within the single amino acids, a group of eight amino acids (Arg, Lys, His, Phe, Tyr, Trp, Val, and Leu) called thereafter "great catchers" could be selected that captured numerous proteins suggesting that they might affect molecular recognition-related processes *in vivo* as well.

Therefore, the rationale for designing the present molecules was to follow a peptide-based strategy to generate relatively small, but bulky, first generation peptide dendrons constructed from three amino acids from the above group: lysine (Lys) with a polar, basic side chain (used here also for the development of a branched structure), and two amino acids with hydrophobic side chains: valine (Val) with a β-branched aliphatic and phenylalanine (Phe) with an aromatic side chain. These dendrons were amphiphilic and exhibited high and variable supramolecular potential in terms of the predominating form of intermolecular interactions: hydrophobic for **D**1 and **D2** and electrostatic and hydrogen bonding for the sinapic acid derivative **D3**. Moreover, as we found previously for compounds of similar architecture, their molecular recognition potential might be enhanced, due to self-assembly into larger aggregates.[10,11] Several other types of much larger branched molecules have been discovered that abolish aggregation of amyloid peptides, for example, polyamidoamine (PAMAM) and polypropyleneimine (PPI),[12] and poly-lysine[13] dendrimers, or show potential in antithrombotic therapy (PAMAM[14] or PAMAM G4-Arginine-Tos[15]). However, densely charged cationic dendrimers may interact with negatively charged blood and cell proteins, and therefore amphiphilic branched peptides hold more therapeutic promise.

Poly-L-lysine (PLL) and poly-L-glutamic acid (PLGA), known for their ability to adopt pH and temperature-dependent, well-defined proteinaceous conformations made them an important model in studying amyloid-related disorders, such as Huntington's, Alzheimer's or Parkinsons diseases.[16,17] Several studies have shown that the aggregation propensity of homo-polypeptides (*e.g.*, polyglutamine, Aib homo-polypeptides, and PLGA) depends on the polypeptide. Moreover, polydispersity of the sample in terms of chain length enhances transformation between unstructured monomeric and structured aggregated forms.[18–21] Here we used polydispersed PLL or PLGA homo-polypeptides for the preparation of proteinaceous secondary structures. Circular dichroism spectroscopy (CD) was used to follow interactions between these polypeptides and the designed dendrons by studying the evolution of the secondary structure-related characteristic bands as a function of dendron concentration. The relative contributions of α-helix, β-sheet, "turn," and "other" secondary structures were estimated using a deconvolution algorithm from the BeStSel program.[22]

It was found that dendrons influenced the resulting CD spectra in a structure- and concentration-dependent fashion. Data deconvolution suggested that, compared to the individual homo-polypeptides, the resulting polypeptide/dendron aggregates exhibited a varying rate of secondary structures, including distorted forms of α-helix, as well as right- and left-hand twisted β-sheet forms in solution, which may indicate a more diffuse structure. Transmission electron microscopy (TEM) images showed that the fibrillation process of polydispersed PLGA in a water solution occurred via self-assembly of microspheres with a particle size distribution ~1 to 5 μm.

2 | RESULTS

2.1 | Synthesis and conformational assignment of dendrons D1 to D3

The general strategy for the synthesis of the **D1** to **D2** dendrons involved application of the active esters method involving coupling in solution of the *N*-orthogonally protected branching unit of the (Lys) Lys(Lys)Phe($C_{12}H_{23}$) structure, (Lys denotes lysine and Phe phenylalanine), with two (**D1**) or four (**D2**) *(N-Cbz)*-protected valines. After Boc-deprotection, dendrons **D1**, and **D2** were obtained. The (Lys) Lys (Lys) Phe fragment of dendron **D3** was synthesized on a solid support using Phe-2chlorotrityl-resin preloaded with phenylalanine. In the final step, N^{ε}-amino groups were acylated with a dimethylformamide (DMF) solution of sinapic acid. The crude products were purified by preparative high-performance liquid chromatography (HPLC) and the

structure was confirmed on the basis of ^{1}H and ^{13}C nuclear magnetic resonance (NMR) (at least 95% purity).

The details of the synthesis and analytical data for dendrons **D1** to **D3** are shown in Schemes 1 and 2 of the Experimental section.

As shown in Figure 1, lipodendrons **D1** and **D2** are amphiphilic due to the presence of cationic amino groups supplemented with two hydrophobic Boc and two Val residues (**D1**) or four Val residues (**D2**) and a dodecyl residue located at the C-terminus. Dendron **D3** is more hydrophilic and prone to extensive intermolecular hydrogen bonding due to the presence of two protonated amino groups and two phenolic OH groups, as well as a carboxyl group located at the C-terminal position. Each dendron was characterized by a structure-specific CD spectrum whose shape and intensity for **D1** and **D2** was concentration-dependent, and for **D3** was concentration insensitive (Figure 2). The CD spectrum for **D2** exhibited two negative bands of low intensity around 205 to 207 and 221 to 223 nm (< 4.8 mdeg for 500 μM). As seen in Figure 3, similar bands are typical for the α-helix conformation. Both **D1** and **D3** exhibited an intense positive band at ~215 to 219 nm (< 15 mdeg for 500 μM). As revealed by CD spectroscopy, apart from their intrinsic chirality, the studied branched peptides self-aggregated, generating a structure-dependent induced CD signal. The propensity for self-assembly was observed before for amphiphilic dendrimeric peptides of similar architecture and is related to their membrane disturbance mechanism.[10,11]

2.2 | Preparation of secondary structures from poly-lysine and poly-glutamic acid commercial samples and their TEM images

The model polypeptides used were commercial samples of PLL hydrobromide and PLGA. These peptides were not monodispersed and contained batch-dependent mixtures of polypeptides varying in chain length and molecular weight (M.W.). (For PLL in the range 10 000-40 000 a.u.; for PLGA >50 000 a.u.) Literature data regarding the generation of random, α-helix, and most of all β-sheet structures from such samples report different conditions[18,20,21,23–26] and therefore, the necessary first step was to establish pH, temperature and

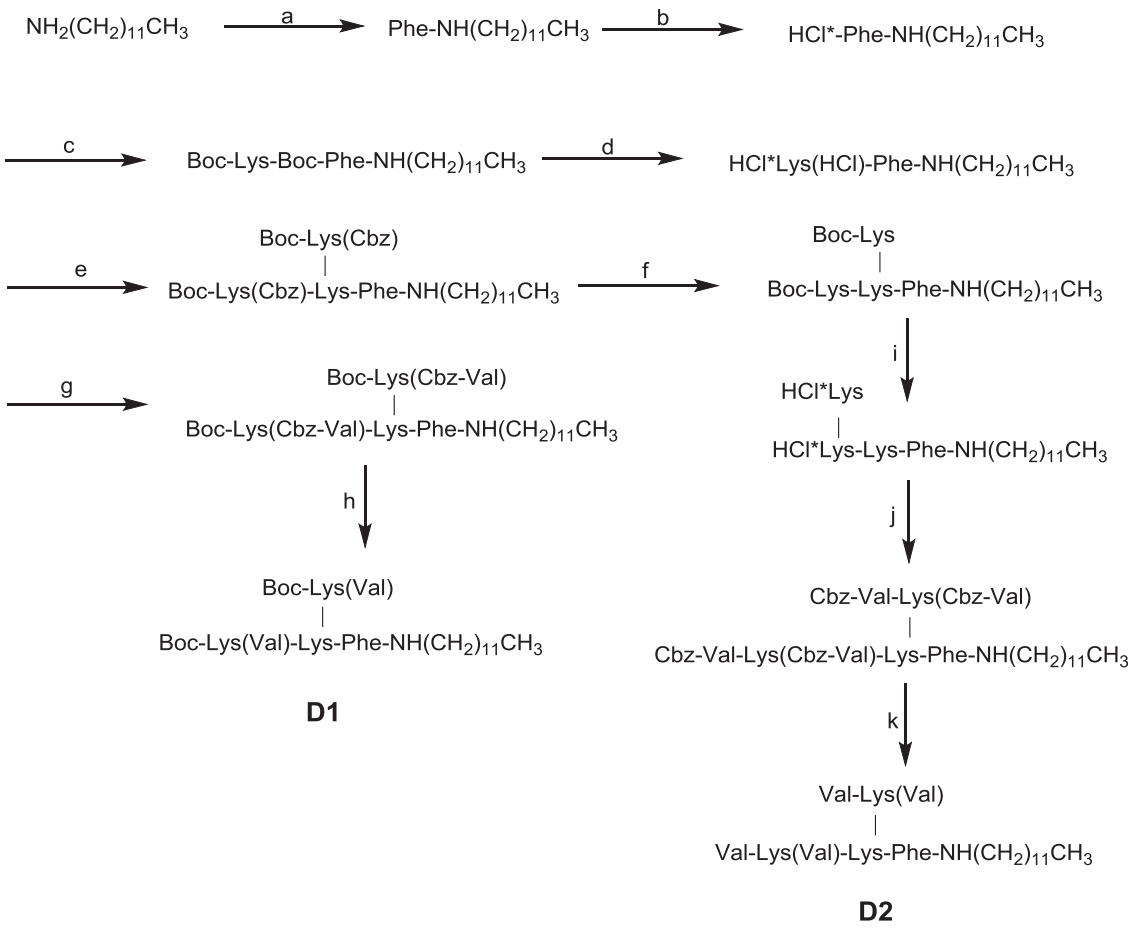

SCHEME 1 Synthesis of dendrons **D1** and **D2** in solution. Reagents and conditions: A, Boc-ROH, DCC/HOSu, DMF, 4 hours at 0 °C to 5 °C and overnight at RT, yield: 95%; B, HCl/AcOEt, overnight at RT, yield 97%; C, Boc-Lys-BocOH, DCC/HOSu, DMF, 4 hours at 0 °C to 5 °C and overnight at RT, yield: 91%; D, HCl/AcOEt, overnight at RT, yield 96%; E, Boc-Lys(Z)OH, DCC/HOSu, DMF, 4 hours at 0 °C to 5 °C and overnight at RT, yield: 89%; F, H_2, Pd/C, MeOH, 6 hours at RT, yield: 85%; G, Cbz-Val, DCC/HOSu, DMF, 4 hours at 0 °C to 5 °C and overnight at RT, yield: 86%; H, H_2, Pd/C, MeOH, 6 hours at RT, yield 75%; I, HCl/AcOEt, overnight at RT, yield 92%; J, Cbz-Val, DCC/HOSu, DMF, 4 hours at 0 °C to 5 °C and overnight at RT, yield: 80%; K, H_2, Pd/C, MeOH, 6 hours at RT, yield 70%. DIC, diisopropylcarbodiimide; DMF, dimethylformamide

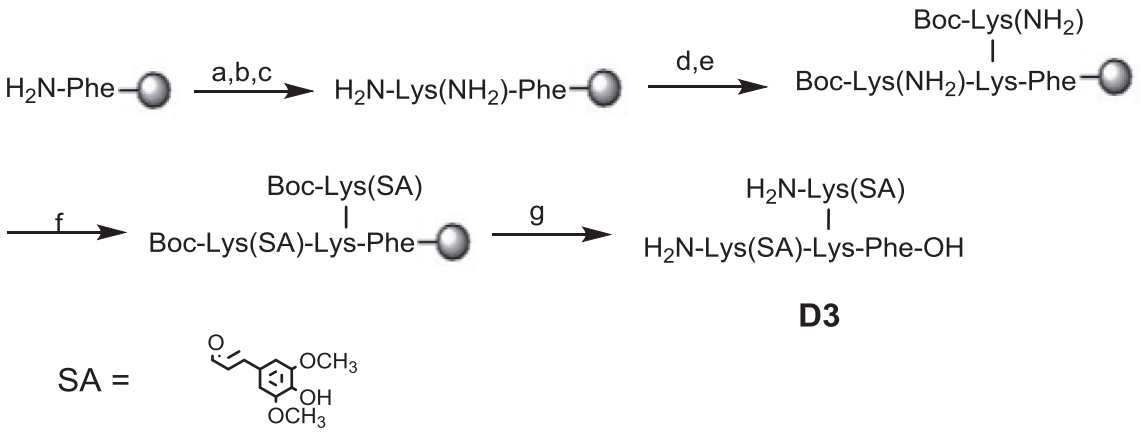

SCHEME 2 Synthesis of dendron **D3** on solid support. Reagents and conditions: A, 20% piperidine, 2 × 5 minutes at RT, B, Fmoc-Lys(Fmoc)-OH, HATU, DIPEA, 4 hours at RT, C, 20% piperidine, 2 × 10 minutes at RT, D, Boc-Lys(Fmoc)-OH, HATU, DIPEA, 4 hours at RT, E, 20% piperidine, 2 × 10 minutes at RT, F, sinapic acid, DIC, Oxyme, DIPEA, 4 hours at RT, G, 50% TFA/DCM, 2 hours at RT. Yield: 18%. DIC, diisopropylcarbodiimide

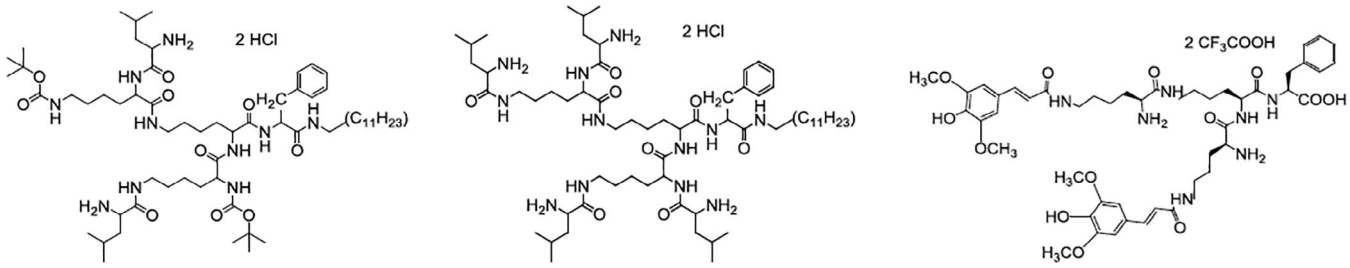

FIGURE 1 Molecular structure of dendrons **D1**-**D3**

time ranges for the formation of a particular secondary structure in solution. According to our experiments, at pH 12, the water solution of PLL revealed a well resolved α-helix conformation, whereas further heating to 52 °C for 15 minutes induced an α-helix to β-sheet transformation (Figure 3). The solution containing the polydispersed PLL sample followed α-helix/β-sheet transformation kinetics observed for the solutions of PLL containing samples of 84 000, 25 500, and 9200 a. u. molecular weight, respectively.[27] On the contrary, the α-helical structure of PLGA in water was prompted by the pH decrease to 4.2, which, when followed by heating the solution to 65 °C for 30 minutes, showed the α-helix to β-sheet transformation. As shown in Figure 4 and S1 the decreased α-helix content and increased β-sheet structure analyzed by the deconvolution program involved an increase of not only a percentage of the β-sheet structure, but also a family of conformations defined as "others" and the appearance of ~10% of turn conformations. Prolonged heating (24 hours) of both polypeptide solutions yielded essentially the same CD profile typical for the β-structure but with lower intensity. Therefore, for studying the interactions of dendrons with the β-structure of polypeptides, the experimental conditions involved the stabilization of primary solutions of dendrons and polypeptides at T > 50 °C or T > 60 °C, respectively for PLL (Figure 3, left) and PLGA (Figure 3, right) and controlling the temperature during CD spectra acquisition by a spectrometer Peltier system.

Rapid CD experiments performed by Mendonça and Hache using a nanosecond 82 MHz titanium-sapphire laser followed the helical fraction evolution during heating a monodispersed PLGA sample (molecular weight 84 000). The authors concluded that only CD at 220 nm is relevant to observe the unfolding of an α-helix and its transformation into the β-sheet form, whereas no change is observed for CD at 204 nm. This observation is in agreement with the present CD data and spectra deconvolution.[28]

An interesting discovery was made when the morphology of 3-month-old solid deposits of both polypeptides in water was observed under a transmission electron microscope. As shown in Figure 5, because of partial water evaporation from the microscope slide, the initially transparent solution containing primary fibrils (pH 4, 25 °C), reaches a critical micelle concentration (CMC) and PLGA (probably in α-helical form) self-assembles into globular aggregates with a particle size distribution ~1 to 5 μm, with the majority of microspheres around 1 μm. A magnified picture of the marked area shows that small microspheres had a tendency for directional aggregation into a fibril-like structure. This unique type of assembly was also revealed in the mature fibers where the microspheres were slightly elongated in a direction perpendicular to the fiber axis. These phenomena were not observed in the PLL solutions, where much smaller nonfibrillar deposits precipitated from the water solution.

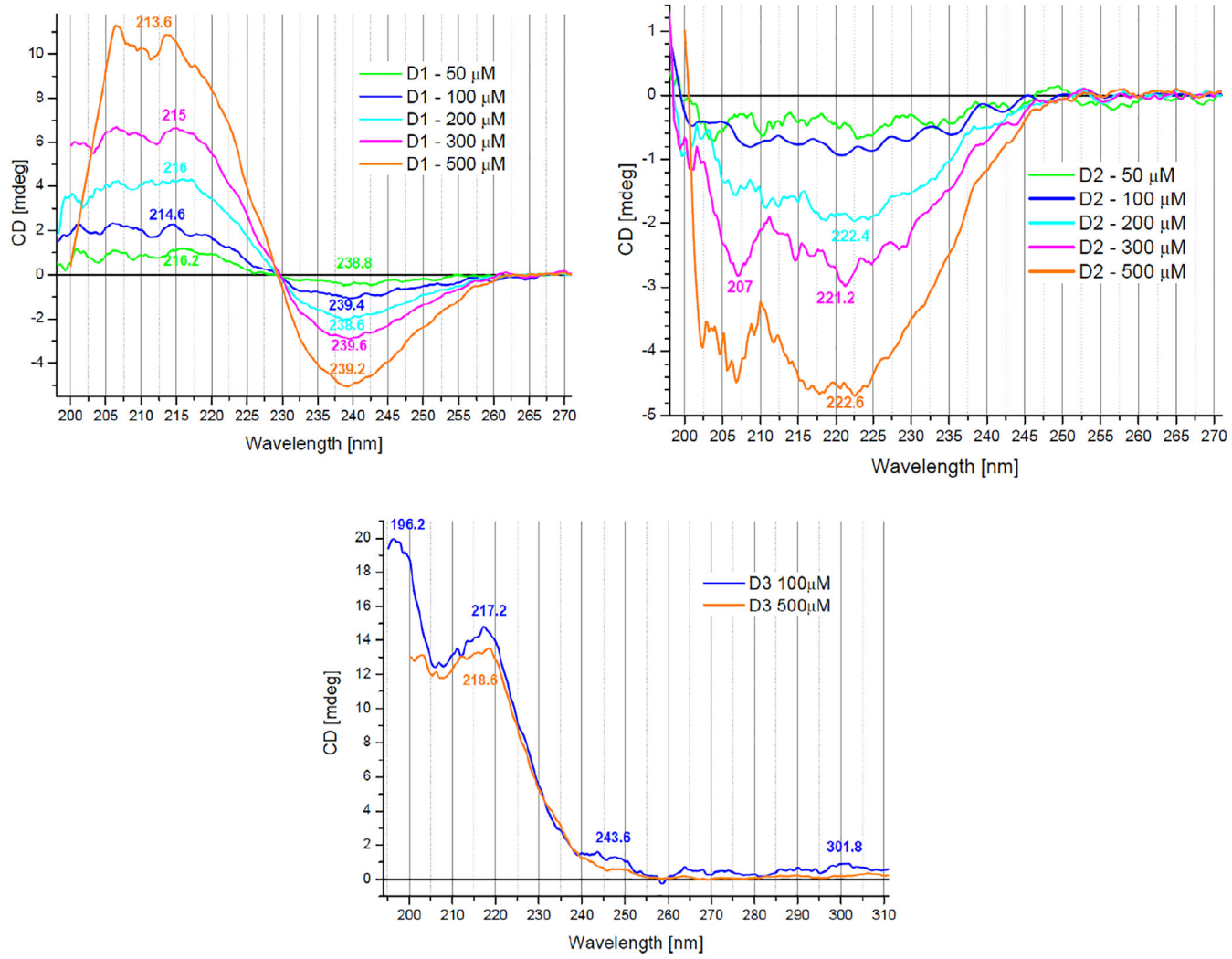

FIGURE 2 CD spectra of dendrons **D1**-**D3** recorded in methanol (spectra not smoothed)

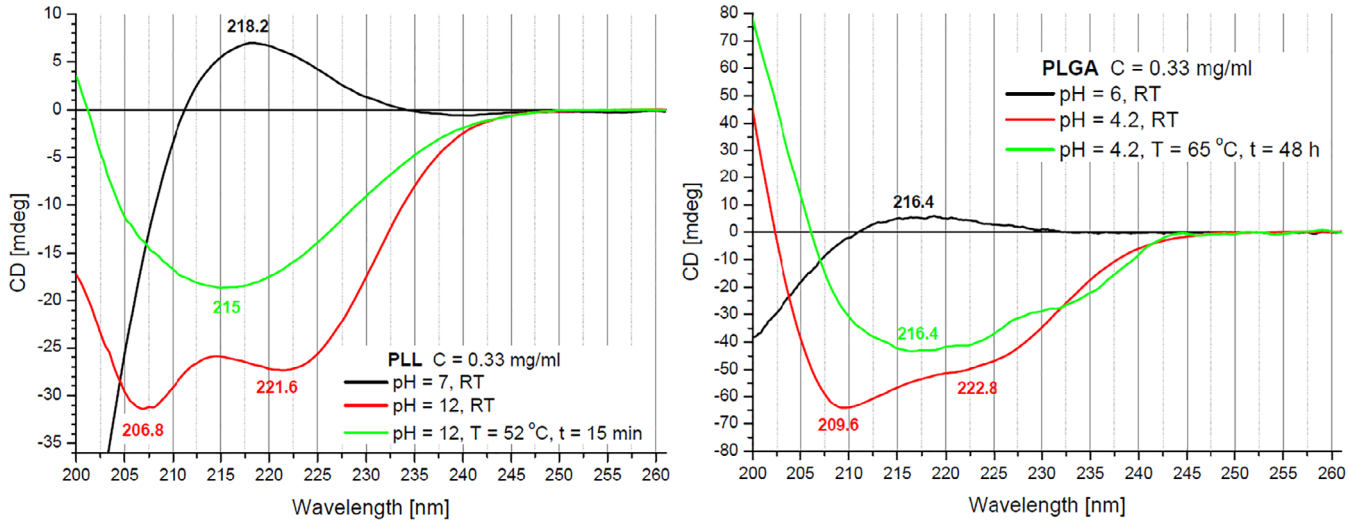

FIGURE 3 CD spectra of PLL and PLGA commercial samples (not smoothed), recorded in pH-adjusted water solutions showing the formation of secondary structures at various temperatures and time of heating. PLL, poly-L-lysine; PLGA, poly-L-glutamic acid

Structural similarity in terms of the advantage of parallel over antiparallel β-sheet subpopulations in the primary PLGA β-sheet model and in amyloid peptides[29] and A$\beta_{1\text{-}40}$ oligomers was also found.[30]

2.3 | Detecting interactions of dendrons with secondary structures of PLL and PLGA by CD spectroscopy

2.3.1 | Interactions of dendrons with an α-helix structure generated from PLL and PLGA

The formation of insoluble fibrillar aggregates rich in β-sheet structure by a normally soluble protein is regarded as a hallmark for a range of diseases including Alzheimer's disease, Parkinson's disease, prion's disease and type II diabetes.[31] In studies related to neurodegenerative diseases, PLL and PLGA often serve as a model of protein aggregation and fibrillogenesis. Among available techniques for the assignment of the existing secondary structures (Fourier-transform infrared spectroscopy, CD, fluorescence spectroscopy, X-Ray, atomic force microscopy and TEM), CD spectroscopy is often used for detecting the *in vitro* secondary structures of peptides and proteins involved in the development and progression of the disease and for studying factors that interfere with this process.[32,33]

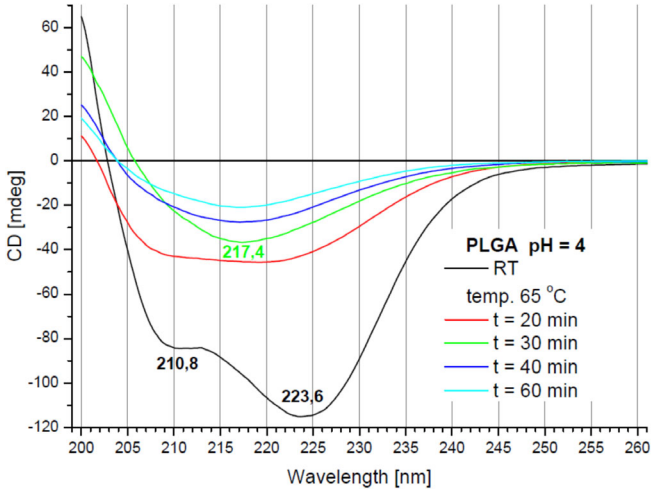

FIGURE 4 Transformation of PLGA α-helix to β-sheet structure upon heating at pH = 4. PLGA, poly-L-glutamic acid

Our studies involved the formation of proteinaceous secondary structures in water solution from polydispersed PLL hydrobromide or PLGA and application of CD spectroscopy for studying their interactions with three rationally designed branched peptides of different structure. Samples used for CD spectra acquisition contained the same amount (μg/mL) of the respective homo-polypeptides and the same volume of dendron solution in an increasing concentration. To diminish the contribution of the original conformation of dendrons to the conformation-characterizing bands of the polypeptides, CD spectra obtained for polypeptide/dendron mixtures were corrected by subtracting the spectrum of the pure dendron at the appropriate concentration.

Conformational transitions were observed as fluctuation of the CD signal in the 200 to 260 nm wavelength range as a function of dendron concentration. The relative contribution of a particular secondary structure can be derived using several algorithms for deconvolution of the experimental CD spectra.[34] For the present studies, deconvolution was carried out with the BeStSel system.[22] This program was specifically designed for handling β-structures of amyloid peptides and other proteins with a high content of the β-sheet structure. Moreover, the program recognized parallel and antiparallel variations of this structure, as well as a twist of the originally planar β-sheet that might be important when the pathway adopted for transformation of the α-helix to the β-sheet structure was of interest.

CD spectra of cationic PLL or anionic PLGA at increasing dendron concentrations are shown in Figures 6–8. Figure 6 presents the impact of dendrons on the α-helical conformation formed by PLL (Figure 6A–C) or PLGA (Figure 6D). Spectra of pure homo-polypeptides had two characteristic negative absorption bands, more intense at ~208 nm and less intense at ~ 222 nm (the respective

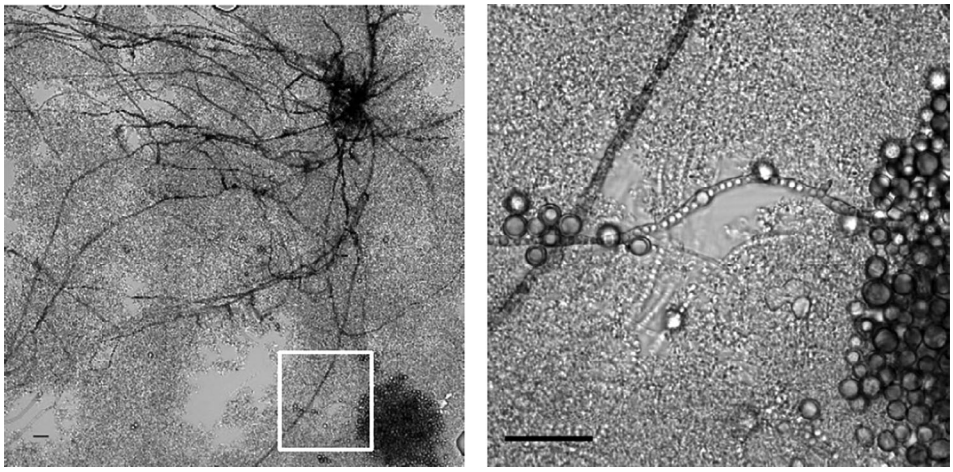

FIGURE 5 Transmission electron scanning microscope image of 3-month-old fibrils of PLGA above the CMC at pH = 4 (left); magnified view of inlet shows the formation of micelles of various sizes and their self-assembly into fibrillar forms (right); scale bar = 20 μm. CMC, critical micelle concentration; PLGA, poly-L-glutamic acid

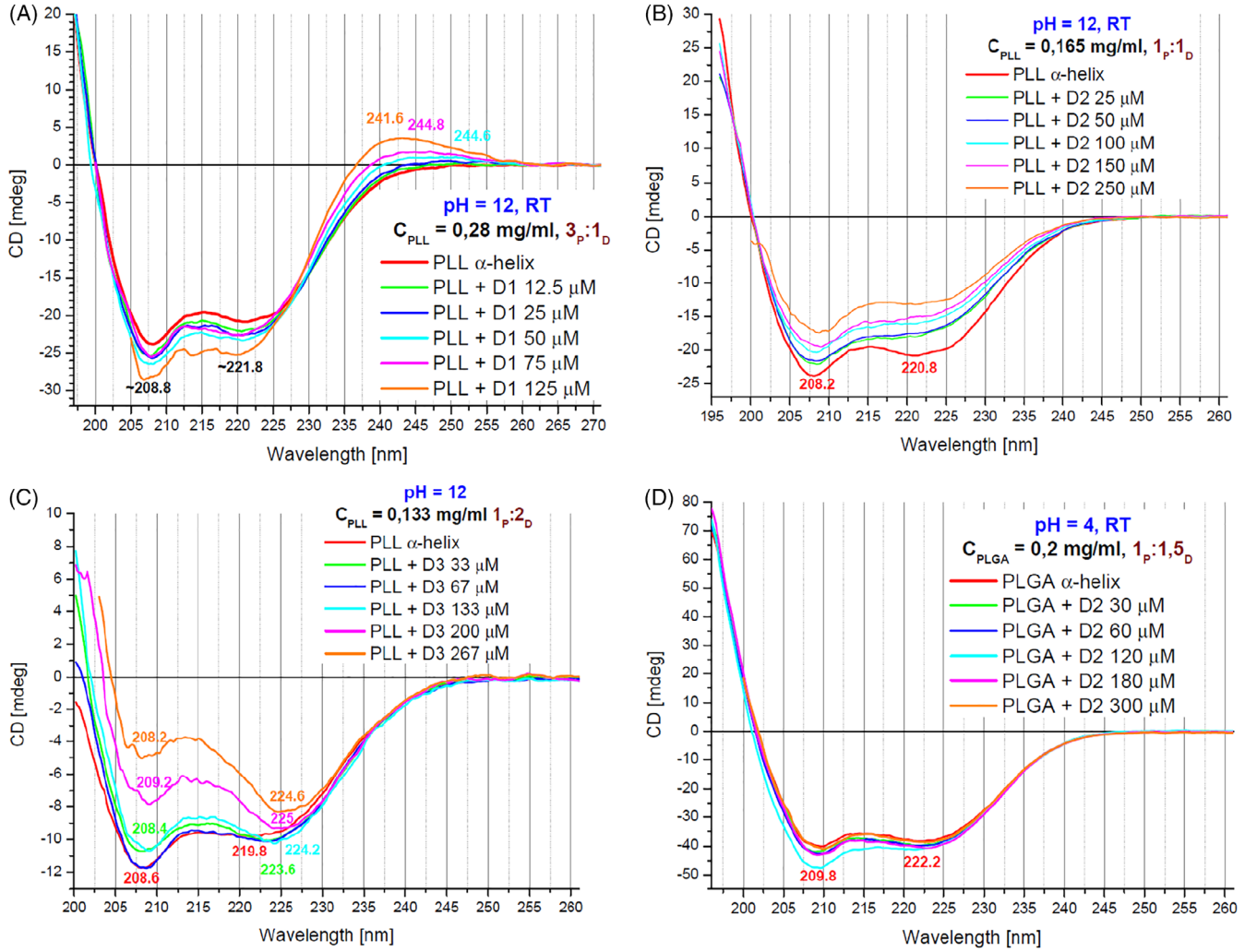

FIGURE 6 CD studies on the influence of dendrons **D1-D3** on preformed α-helix secondary structures generated from polycationic PLL, A-C, and polyanionic PLGA, D, upon addition of an increasing amount of dendron (inlets show effective dendron concentrations after dilution). CD, circular dichroism; PLL, poly-L-lysine; PLGA, poly-L-glutamic acid

$\pi \rightarrow \pi^*$ and $n \rightarrow \pi^*$ transition), corresponding to the α-helix of the peptide bond (red line). The PLL intensity, but not the position of the characteristic bands, slightly fluctuated when titrated with **D1** and **D2** at higher concentrations, suggesting that the resulting intermolecular interactions were weak. More significant was the impact of sinapic acid functionalized **D3**. After the addition of **D3** above a concentration of 133 μM, a decrease in intensity in λ = 208 nm was observed that was not associated with the corresponding changes in λ = 222 nm. Such changes were often related to fluctuation in "turn" structure content, since it had a maximum at this wavelength.

The surface of PLGA molecules in either form was, at least in part, negatively charged in a pH-dependent manner or contained neutral carboxyl groups. Therefore, it was expected that the influence of relatively small positively charged dendrons on the α-helix and β-sheet structures of PLGA (M. W. >50 000 a.u) might be insignificant. Indeed, dendrons **D1** to **D3** had almost no impact on the α-helical conformation formed by PLGA, with only a small intensity fluctuation in the CD curve, as shown for the representative dendron **D2** (Figure 6D and Table 1). This observation is in agreement with the results of rapid CD experiments performed by Mendonça and Hache for monodispersed PLGA sample (molecular weight 84 000).[28]

Populations of secondary structures detected during titration of PLL or PLGA in the α-helix conformation with dendrons were calculated by the BeStSel program and are shown in Table 1. The results revealed that the prevailing α-helix structure and a small amount of β-sheet, as well as a significant amount of β-turn (10%-20%), and conformations defined as "others" were present in the primary solution. Upon the addition of a small quantity of **D1** to **D3** dendrons to the PLL solution, the amount of regular α-helix was slightly decreased, whereas the amount of the distorted form was conserved. Addition of 75 μM of **D1** or **D2** resulted in an increase of the total amount of the β-sheet structure, up to ca 21%, with a concomitant decrease of the range of structures defined as "others." Interestingly, only "relaxed" and "right-hand-twisted" but not "left-hand twisted" β-sheet forms of PLL were observed. Titration with **D3** at 200 and 266 μM had a more significant impact; the initial content of regular and distorted α-helix

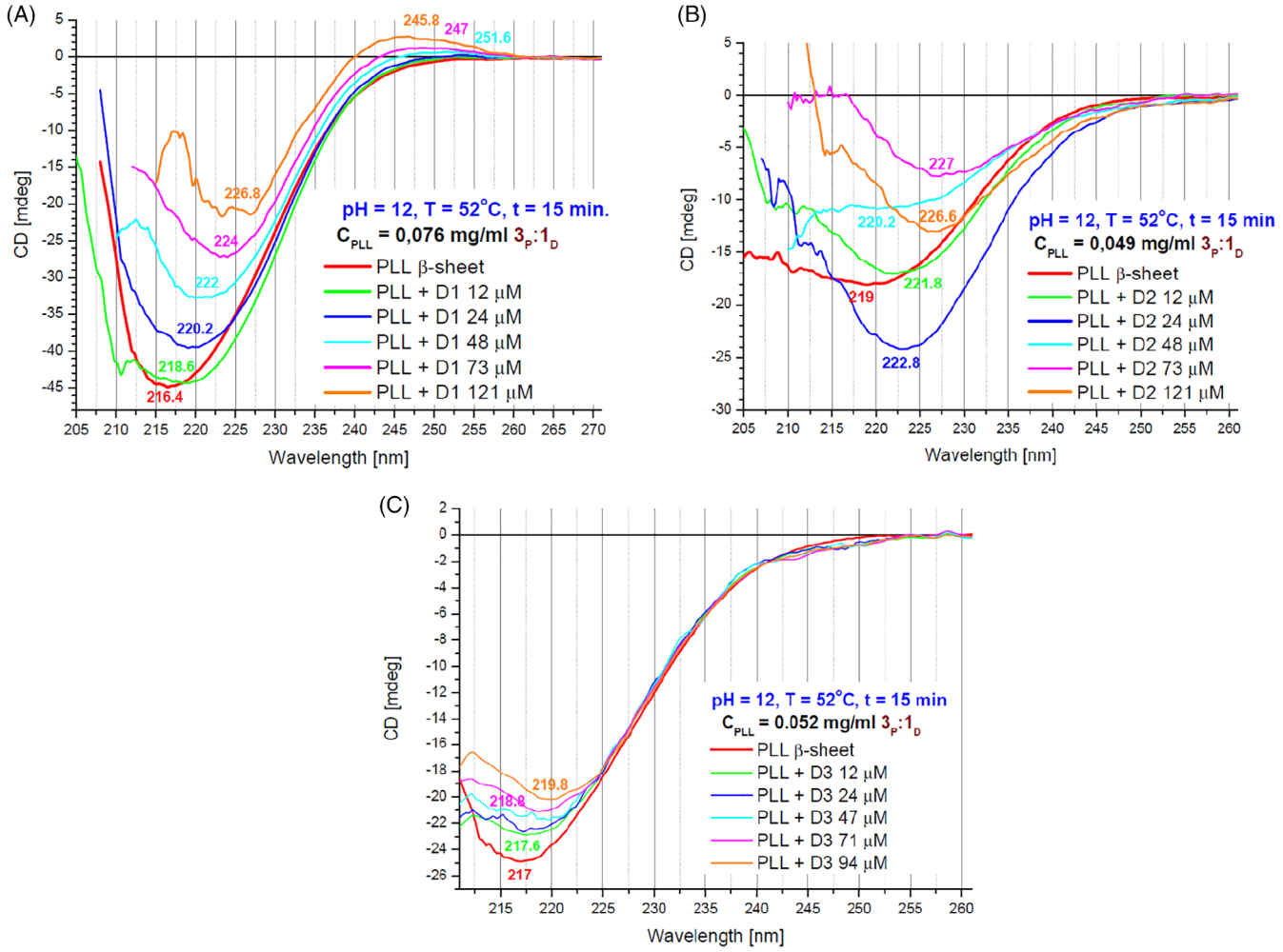

FIGURE 7 CD studies on the influence of **D1-D3** dendrons on β-sheet structures generated from polycationic PLL. CD, circular dichroism; PLL, poly-L-lysine

was reduced from ~70% to 75% to ~55%. The interrelation between the β-turn and β-sheet structures was interesting. Increasing the **D3** concentration to 133 μM resulted in the sudden increase of β-turn content to ~21%, whereas at 200 μM, almost all the β-turn forms were converted into the β-sheet form. Doubling the **D3** concentration to 266 μM resulted in the decreased content of the β-sheet form to 11%, with an increase in the β-turn content to ~ 32%. This may suggest that upon interaction with amphiphilic **D3**, either longer PLL chains became bent or **D3** is connected to the C-terminal fragments of two α-helices via formation of multiple hydrogen bonds and electrostatic interactions. Both structures in the next step may have facilitated or strengthened the existing β-sheet pattern.

2.3.2 | Interactions of dendrons with the β-sheet structure generated from PLL and PLGA

The influence of dendrons on the β-sheet conformation formed by PLL and PLGA homo-polypeptides in the absence and presence of dendrons is shown in Figures 7 and 8, respectively. Micsonai *et al*. showed by analysis of the CD spectra and the respective molecular conformations for proteins deposited in the Protein Data Base, these containing ca 50% α-helix show similar CD curve profiles, whereas those having *ca* 50% β-sheet, even with negligible α-helical content, show CD spectra with diverse amplitudes.[35]

Indeed, titration of PLL in the β-sheet conformation by **D1** and **D2** resulted in a lowered intensity, more discrete structure and a shifted position of the negative band at 216 to 219 nm to a higher wavelength (~227 nm) (Figure 7AB). Moreover, even shifts in the CD trace for most wavelengths were observed only upon titration with **D1**, but not **D2**. The impact of dendron **D3** on the β-sheet structure of PLL was much smaller in terms of reducing the band intensity and shifting the band position (Figure 7C). CD spectra deconvolution in the case of **D3** (Table 2) showed a decrease in the β-sheet content in favor of an α-helix and a significant increase of structures defined as "others" (up to 52%-59%). Spectral deconvolution can give reliable results when the measured CD spectra are at least in the 200 to 250 nm λ range.[22] For this reason, calculations for several CD

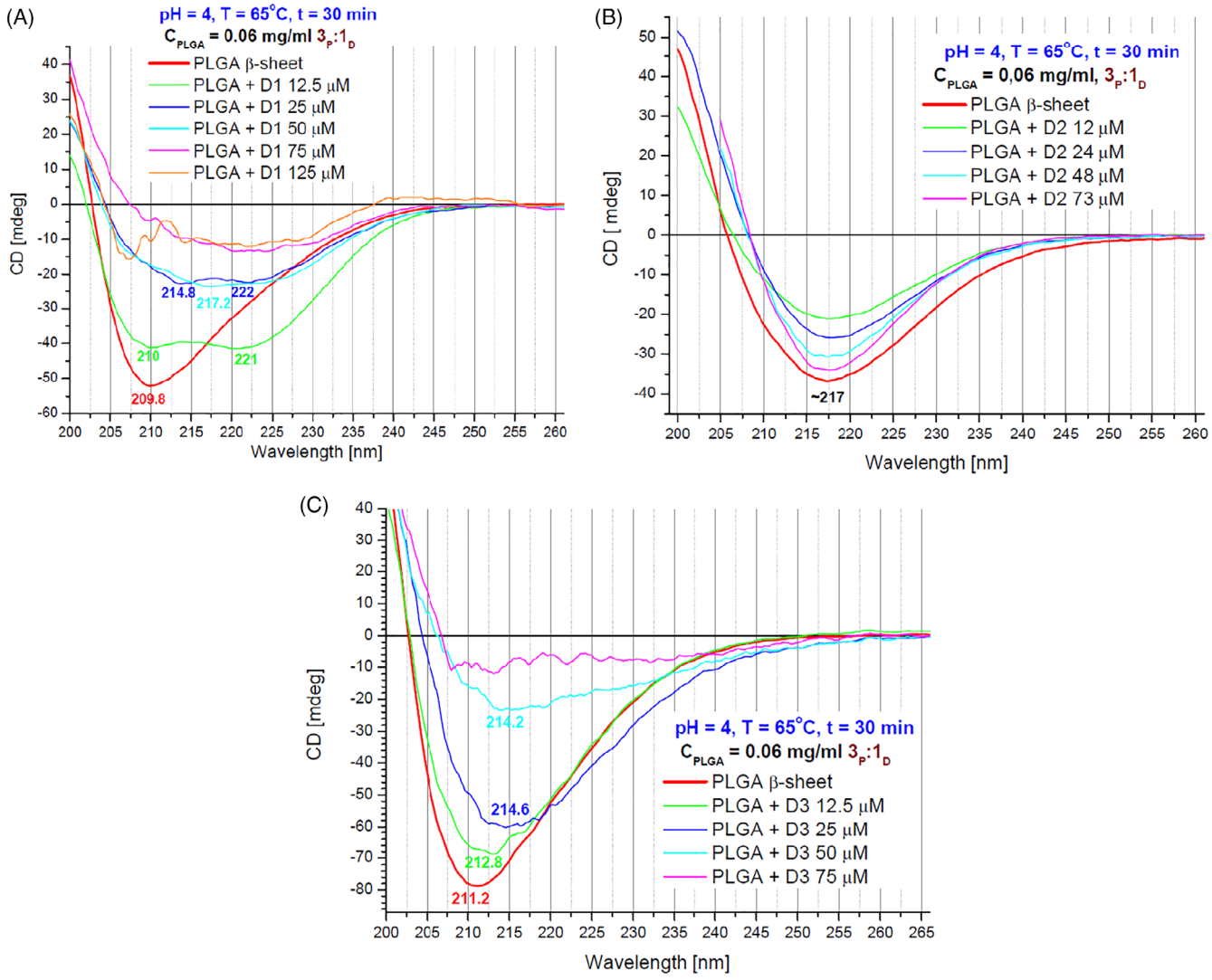

FIGURE 8 CD studies on the influence of **D1-D3** dendrons on the β-sheet structure generated from polyanionic PLGA. CD, circular dichroism; PLGA, poly-L-glutamic acid

spectra measured above 205 nm could not be performed: the entire entry from Figure 7A,B: (PLL-β-sheet + **D1**) and (PLL-β-sheet + **D2**) and those of higher concentrations of PLGA β-sheet + **D2** (Figure 8B).

CD spectra deconvolutions calculated by the BeStSel program (Table 2) showed that the total amount of the generated β-structure in primary solution depended on the type of polypeptide. It was around 46% for PLL, and only 24% to 33% in experiments involving PLGA titrated with **D1**, **D2**, and **D3**, respectively. Primary solutions of both homo-polypeptides expressed an advantage of parallel over anti-parallel β-sheet conformations, and the presence of a significant amount of structures defined as "others" (45%-54%) and ~ 10%) of β-turn structures.

As shown in Figure 8A-C, dendrons show structure-dependent behaviour. From visual assignment, dendrons **D1** and **D2** interacted in a different way with PLGA formatted to the β-sheet form. Dendron **D1** (2 Val and [+2] charge) in the 12.5 to 25 μM concentration range showed the appearance of an α-helix. Above a concentration of 50 μM, spectra exhibited lower intensity and discrete structures. According to the deconvolution procedure, this accounted for the development of a range of conformations defined as "others" (~44%). At 125 μM, the CD curve showed a new minimum at 207 nm (Figure 8A). Structure deconvolution for this concentration revealed an increase in "turn" (~21%) and β-sheet (~32%) content and a decreased percentage of conformations defined as "others" (~32%). Dendron **D2** [4 Val and (+) 4 charge] showed only a small fluctuation in intensity but not in the positioning of the negative band at 217 nm (Figure 7C), thus suggesting structural cooperativity with the β-sheet structure. In contrast, dendron **D3** at a higher concentration changed the shape, intensity, and structure of the CD trace in a concentration-dependent manner. At 75 μM, the CD trace had the shape of a wide plateau and a discrete structure with the intensity approaching zero. However, reduction of the twisted and a higher percentage of the relaxed β-sheet form might suggest a stabilizing effect of **D3**. Interestingly, the observed differences in the shape and bands intensity of the CD spectra were not reflected by spectra deconvolution, since only several percentage

TABLE 1 Populations (%) of secondary structures observed in solution of PLL or PLGA in α-helix form upon addition of increasing concentrations of dendrimers

	α-Helix (%)		β-Sheet (%)					
			Antiparallel					
α-helix Denrimer/conc. (μM)	Regular	Distorted	left-H	relaxed	right-H	parallel	Turn (%)	Other (%)
PLL	25.4	14.0	0	6.2	0	1.5	15.2	37.6
PLL + D1/12	27.0	13.2	0	11.5	0.2	0	14.0	34.1
PLL + D1/25	25.7	14.8	0	0	7.1	0	15.2	37.2
PLL + D1/50	28.8	14.8	0	0	12.4	0	15.5	29.3
PLL + D1/75	23.5	12,0	0	21.3	0	0	14.4	28.3
PLL	25.4	14.0	0	6.2	0	1.5	15.2	37.6
PLL + D2/12	19.9	12.2	0	7.2	8.2	4.3	12.4	35.7
PLL + D2/25	19.0	12.6	0	3.3	8.0	4.5	14.4	38.2
PLL + D2/50	29.8	11.4	0	6.3	8.5	3.8	12.8	38.7
PLL + D2/75	18.9	11.3	0	5.0	11.7	2.7	12.7	37.8
PLL α-helix	55.2	20.3	0	0	0	0	6.6	18.0
PLL + D3/33	51.5	20.0	0	0	0	0	10.0	18.5
PLL + D3/66	54.8	18.1	0	0	13.9	0	10.0	11.0
PLL + D3/133	52.4	20.0	4.1	0	0	0.8	22.7	0
PLL + D3/200	46.2	15.6	0	0	19.8	0	1.4	17.0
PLL + D3/266	33.9	20.7	0	0	11.0	0	31.9	2.5
PLGA α-helix	48.5	19.7	0	0	3.4	0	10.6	17.9
PLGA + D2/30	51.3	20.1	0	0	3.2	0	9.9	15.4
PLGA + D2/60	51.1	20.1	0	0	1.8	0	9.8	17.2
PLGA + D2/120	50.4	20.5	0	0	4.1	0	6.7	18.2
PLGA + D2/180	50.4	20.2	0	0	1.9	0	9.6	18.0
PLGA + D2/266	49.8	20.2	0	0	1.5	0	10.3	18.2

Abbreviations: PLL, poly-L-lysine; PLGA, poly-L-glutamic acid.

fluctuations from the initial content of the secondary structures were found (Table 2). One of the possible reasons is that it is hard to interpret the "not classic" shape of the CD trace and the fact that the development of deconvolution procedures are still mostly based on databases of larger well-ordered proteins.[36]

The amphiphilic dendrons **D1** to **D3**, in addition to their intrinsic chirality, had the ability to self-assemble and therefore, to form secondary structures which generated an induced CD signal. Due to intermolecular interactions dominated by electrostatic and hydrogen bond forces, aggregated particles influenced the populations of the secondary structures formed by the homo-polypeptides PLL and PLGA in a structure- and concentration-dependent manner. Conformational transitions were followed by the evolution of the CD signals at structure-characteristic wavelengths (α-helix, β-turn, β-sheet, etc.) as a function of dendron concentration. CD spectra of several polypeptide/dendron mixtures were considerably different from those corresponding to the individual polypeptides. The highest impact of dendrons was visualized by the reduction of the intensity, discrete structure, and dislocation of characteristic bands in the CD spectra. CD spectra deconvolution showed that, in fact, complex mixtures of interacting polypeptides and dendrons were formed with variable conformation rates. In particular, the observed fluctuation between relaxed, parallel and antiparallel right- and left-hand shifted β-sheet may introduce "chiral noise" to the intensity and fine structure of the CD signal. The highest impact on the α-helix structure formed by PLL (pH 12) had dendron **D3**, whereas all cationic dendrons had little impact on the α-helix structures formed by polyanionic PLGA (pH 4). However, addition of the structurally different dendrons **D1** and **D3** influenced the shape, intensity, and band position in the CD spectra of PLGA in the β-sheet conformation. Dendron **D2** bearing four cationic centres flanked by bulky valine, dodecyl and *tert*-butoxycarbonyl (Boc) groups affected the secondary structure composition to a lesser degree, probably due to inhibition of the generation of multiple hydrogen bonds.

Supramolecular mechanisms for dendron-polypeptide interactions considering single dendron molecules could be different from variations of capping-related mechanisms proposed by Klainert *et al*., for explaining the decomposition of fibrillar forms of Aβ peptides by third-generation PPI or third- to fifth-generation PAMAM dendrimers.[12,37] First, the PPI and PAMAM dendrimers used in

TABLE 2 Populations (%) of secondary structures observed in solution of PLL or PLGA in β-sheet form upon addition of increasing concentrations of dendrimers

	α-Helix (%)		β-Sheet (%)					
			antiparallel					
Polypeptide+ dendrimer	regular	distorted	left-H	relaxed	right-H	parallel	Turn (%)	Other (%)
PLL β-Sheet Denrimer/conc. (μM)	0	2.3	0	7.3	8.9	29.6	5.5	46.3
PLL + D3/12	8.5	2.2	0	11.5	0.2	0	14.0	41.8
PLL + D3/24	21.7	12.8	0	9.1	0	0	11.4	45.0
PLL + D3/47	20.9	11.3	0	0	8.6	0	11.1	48.1
PLL + D3/74	12.1	2.3	0	0	10.4	15.9	9.0	59.7
PLL + D3/94	2.3	4.8	0	1.9	11.2	16.9	10.5	52.5
PLGA β-Sheet	4.0	5.6	4.7	4.1	0.6	14.7	12.1	54.2
PLGA + D1/12	19.6	12.1	0	6.4	6.9	7.7	13.4	33.9
PLGA + D1/25	2.9	7.2	0	9.7	3.3	0	13.7	41.4
PLGA + D1/50	0	5.4	0	13.2	1.9	11.9	16.0	44.7
PLGA + D1/75	4.7	3.9	9.8	18.9	7.3	0	12.0	42.9
PLGA + D1/125	3.8	4.8	2.6	17.0	15.4	0	21.2	35.1
PLGA β-Sheet	27.4	4.9	0	0	0	29.1	2.9	40.5
PLGA + D2/12	1.8	5.1	7.8	15.3	3.1	14.9	8.7	43.3
PLGA + D2/24	0	0.5	8.2	9.5	0	34.0	7.4	40.5
PLGA β-Sheet	5.9	6.2	3.4	18.6	11.2	0	13.0	41.6
PLGA + D3/12	6.0	5.1	4.6	17.1	12.1	0	13.4	41.7
PLGA + D3/25	1.7	3.9	2.3	19.8	13.3	1.7	11.4	45.7
PLGA + D3/50	0	3.3	2.7	19.1	12.9	0	13.6	48.5
PLGA + D3/75	2.3	2.8	5.5	18.2	14.4	0	13.4	43.4

Abbreviations: PLL, poly-L-lysine; PLGA, poly-L-glutamic acid.

those studies were relatively large, polycationic compounds bearing on the surface 16 to 128 amino groups enabling the formation of an extensive system of multiple hydrogen bonds and electrostatic interactions with the existing of Aβ fibrils. In contrast, the presently studied dendrons were much smaller molecules with only (+) 2 or (+) 4 charges. However, their amphiphilic structure enabled by the presence of cationic centers and several lipophilic groups might be advantageous in the creation of multiple interactions with the existing secondary structures. Moreover, as revealed by CD spectroscopy, as a part of their intrinsic chirality, the studied branched peptides self-aggregated generating structure-dependent induced CD signals. Such behavior is characteristic of natural antimicrobial peptides that make large deposits on negatively charged microbial membranes.[38]

3 | EXPERIMENTAL

3.1 | Materials

All solvents and reagents were of analytical grade and were used without further purification. All reagents and solvents were obtained from Sigma-Aldrich. Mass spectra were recorded with a Mariner electrospray ionization (ESI) time-of-flight mass spectrometer (PerSeptive Biosystems) for the samples prepared in methanol (MeOH). The ^{1}H-NMR spectra were recorded using a Bruker Avance spectrometer at 500/125 using deuterated solvents and TMS as an internal standard. Chemical shifts are reported as δ values in parts per million, and coupling constants are given in hertz. Thin layer chromatography (TLC) was performed on aluminium sheets with the silica gel 60 F254 from Merck. Column chromatography (CC) was carried out using silica gel (230-400 mesh) from Merck or Sephadex LH20. The TLC spots were visualized by treatment with 1% alcoholic solution of ninhydrin and heating. PLL hydrobromide (M.W. 4000-20 000) and PLGA (M.W. > 50 000) were obtained from MP Biomedicals. MeOH, sodium hydroxide, and hydrochloric acid were purchased from Sigma-Aldrich. Water solutions of both polypeptides were pH-adjusted with HCl or NaOH solutions and controlled by a Mettler-Toledo pH-meter.

3.2 | Sample preparation

Stock solutions of **D1** to **D3** (1 mM) were prepared by dissolving the respective sample in MeOH. The solutions were stored at room temperature (RT).

Polypeptides (2 mg/mL) were obtained by dissolution in distilled water and then diluted to the appropriate concentration. The proper dilution was determined on the basis of the high tension (HT) value, which was determined during the CD measurement. The HT should not be higher than 600 V (lower concentration = lower HT). The correct pH for a given peptide was obtained by adding NaOH to PLL (pH 12) and HCl to PLGA (pH 4), respectively. The pH value was measured using a LE438 electrode with a built-in temperature sensor connected to a Mettler-Toledo FiveGo pH meter. The peptides thus prepared were mixed with methanolic dendron solutions at a suitable rate.

3.3 | Synthesis and spectroscopic data of dendrons D1 to D3

Peptide dendrons were obtained using the active esters method as shown in Scheme 1. The substrate with free amino groups was dissolved in MeOH, and then 50% excess of corresponding active ester in MeOH was added successively. The reaction was carried out at RT for 5 days, then the solvent was evaporated to dryness and the post-reaction mixture was dissolved in MeOH. The compounds were purified on a Sephadex LH-20. Then, the solvent was removed in vacuo resulting in the title compound as lightly yellow oil.

The synthetic pathway for dendrons **D1** and **D2** is shown in Scheme 1.

Dendron **D1:** $C_{59}H_{106}N_{10}O_{10}$, M.W. 1115.53, Exact Mass: 1114.81, m/z: 1114.81, Elemental Analysis: C, 63.52; H, 9.58; N, 12.56; O, 14.34; MS (ESI, MeOH): m/z: 1138[M + Na]$^+$.

^{1}H NMR (500 MHz, MeOD), δ: 0.75 to 0.85 (m, 9H, C**H$_3$** DDA, 2xC**H$_3$** Val), 1.2 to 1.9 (m, 62H, 3xβC**H$_2$** Lys, 3xγC**H$_2$** Lys, 3xδC**H$_2$** Lys, 2xβC**H$_2$** Val, 2xC[C**H$_3$**]$_3$, C**H$_2$** C$^{2\text{-}11}$ DDA), 2.5 to 2.8 (m, 10H, 3xεC**H$_2$** Lys, βC**H$_2$**-Phe, C**H$_2$** C^1 DDA), 2.9 to 3.1 (m, 4H, 2xC**H$_2$** Val), 3.9 to 4.3 (m, 6H, 3xαC**H** Lys, αC**H** Phe, 2xαC**H** Val), 7.3 to 7.65 (m, 5H, **H**-Ar-Phe).

Dendron **D2**: $C_{59}H_{108}N_{12}O_8$, M.W. 1113.56, Exact Mass: 1112.84, m/z: 1112.84, Elemental Analysis: C, 63.64; H, 9.78; N, 15.09; O, 11.49; MS (ESI, MeOH): m/z: 1114[M + H] $^+$.

^{1}H NMR (500 MHz, D_2O), δ: 0.7 to 0.9 (m, 15H, C**H$_3$** DDA, 4xC**H$_3$** Val), 1.2 to 2.1 (m, 48H, 3xβC**H$_2$** Lys, 3xγC**H$_2$** Lys, 3xδC**H$_2$** Lys, 4xβC**H$_2$** Val, C**H$_2$** C$^{2\text{-}11}$-DDA), 2.7 to 3.0 (m, 12H, 3xεC**H$_2$** Lys, 2xβC**H$_2$** Phe, C**H$_2$** C^1-DDA), 2.8 to 3.1 (m, 8H, 4xC**H$_2$** Val), 3.9 to 4.5 (m, 8H, 3xαC**H** Lys, αC**H** Phe, 4xαC**H** Val), 7.15 to 7.6 (m, 5H, **H**-Ar Phe).

*Synthesis of dendron **D3** on solid support*

Fmoc-protected Phe-2chlorotrityl-resin (resin preloaded with phenylalanine) (1 g; equiv. 0.82 mmol/g) was swollen in DMF for 2 hours. The Fmoc group was removed using two 5 minutes treatments with 2:8 piperidine/DMF, and washed thoroughly with DMF. Once drained, the resin was acylated with a solution containing Fmoc-Lys (Fmoc) OH (0.775 g; 1.3 mmol)), [2-(7-Aza-1H-benzotriazole-1-yl)-1, 1, 3, 3-tetramethyluronium hexafluorophosphate] (HATU; 0.973 g; 2.56 mmol), and N, N-Diisopropylethylamine (DIPEA; 0.827 g; 6.4 mmol) in anhydrous DMF for 4 hours at RT. After being drained and washed with DMF, the Fmoc group was removed, as previously described. After draining the resin, the acylation procedure was repeated for 4 hours with a solution containing Boc-Lys (Fmoc) OH (1.2 g; 2.56 mmol), HATU (1.946 g; 5.12 mmol), and DIPEA (1.65 g; 12.77 mmol) in anhydrous DMF. After being drained and washed with DMF, the Fmoc group was removed and the resin was washed with DMF. The last acylation procedure was performed for 4 hours with a solution of sinapic acid (0.574 g; 2.56 mmol), diisopropylcarbodiimide (DIC) (0.646 g; 5.12 mmol), Oxyme (0,727 g; 5.12 mmol), and DIPEA (1.65 g; 12.77 mmol) in anhydrous DMF. After being drained and washed with DMF, the peptide-resin was deprotected and released by treatment with a TFA/DCM (5:5) solution at RT for 2 hours. The resin was filtered off and washed with ethyl acetate. The volatiles were then removed in vacuo, and the crude product **D3 was** precipitated twice with diethyl ether. The crude product **D3** was purified by preparative HPLC using a C_{18} column, 250 × 21.20 mm, particle size 15 μm and a pore diameter of 300 Å. The mobile phase consisted of a gradient from 5% to 95% MeOH/H_2O, 0.05% HCl, at a flow rate of 3.0 mL/min. Final yield: 18%. The synthetic pathway for dendron **D3** is shown in Scheme 2.

Dendron **D3:** $C_{49}H_{67}N_7O_{13}$, M.W. 962.11, Exact Mass: 961.48, m/z: 962.6, Elemental Analysis: C, 61.17; H, 7.02; N, 10.19; O, 21.62; MS (ESI, MeOH): m/z: 984.6 [M + Na] $^+$, 962.6 [M + H] $^+$.

^{1}H NMR (600 MHz, MeOD), δ: 1.23 to 1.98 (m, 26H, 3xβC**H$_2$** Lys, 3xγC**H$_2$** Lys, 3xδC**H$_2$** Lys, 3xεC**H$_2$** Lys, βC**H$_2$** Phe), 2.97to 3.25 (m, 2H, 2xαC**H** Lys), 3.35 to 3.41 (m, 2H, αC**H** Phe, αC**H** Lys), 3.86 to 3.96 (m, 12H, 4xOC**H$_3$** sinapic acid), 6.37 to 6.54 (m, 8H, 4x**H**-Ar sinapic acid, 2x—C**H**=C**H**— sinapic acid), 6.85 to 6.95 (m, 9H, 5xεN**H** Lys, 2xαN**H$_2$** Lys), 7.12 to 7.36 (m, 5H, **H**-Ar Phe), 7.40 to 7.51 (m, 2H, 2xO**H** sinapic acid).

3.4 | Circular dichroism measurements

During conformational studies on the influence of the **D1** to **D3** dendrons on the α-helix structure generated from PLL or PLGA, CD spectra were measured at RT with a Jasco J-715 spectropolarimeter using a 0.2 cm path length quartz cuvette and (1:1, 1:2) vol/vol ratio between peptide and dendron. The HT of the anode did not exceed 600 V. For studies concerning their impact on the β-sheet structure, CD spectra were collected with a Jasco J-815 spectropolarimeter fitted with a Peltier temperature controller, using a rectangular quartz cuvette with a fitted cap and an optical path length of 1 to 0.2 cm and (3:1) vol/vol ratio between peptide and dendron. CD measurements were performed after the samples had been heated to the appropriate temperature at a given time. PLL creates a β-sheet structure after 15 minutes at 52 °C and PLGA after 30 minutes at 65 °C. Samples of both polypeptides were dissolved in water with the addition of HCl or NaOH for pH adjustment, whereas dendrons were dissolved in MeOH.

The β-sheet structure cell conditioning at the appropriate temperature by the spectrometer Peltier system was continued for 15 minutes. Then, the same volume of MeOH solution of dendrons at the appropriate temperature and concentration was added to the cell and the CD spectrum was measured after ca 5 minutes. All spectra were averaged over at

least five scans and baseline-corrected with a mixture of water with an appropriate pH and MeOH as the reference. To diminish the contribution of the original conformation of dendrons to the conformation-characterizing bands of the polypeptides, the CD spectra obtained for the polypeptide/dendron mixture were corrected by subtracting the spectrum of the pure dendron at the appropriate concentration.

3.5 | TEM

PLGA fibrillation was observed under a LSM780/Elyra PS.1 (Zeiss) electron microscope in transmission mode. Objects were registered using transmitted light and ZEN 2012 (Zeiss) and the ×40 objective with a ×10 ocular set-up. All images were supplemented with a scale bar = 20 μm.

4 | CONCLUSIONS

Aggregation is a multistep process where monomers arrange into oligomers, protofibrils, and mature fibrils. Preventing the formation or disassembly of either oligomers or fibrils is, at present, one of the main efforts in drug discovery. Involvement of natural compounds in the regulation of this process has been documented. Therefore, the design and detailed study of the aggregation process in the presence of new molecular entities is one of the possible avenues to achieve better therapeutics.

The CD spectra reveal that the small branched peptides carrying several valine or sinapic acid residues significantly altered the secondary structures of PLL and PLGA model polypeptides in a structure- and concentration-dependent fashion. The amphiphilic character, high supramolecular capacity, and probable self-aggregation into larger nanoparticle structures are structural factors that enabled multiple contacts with polypeptides. In several cases, the CD spectra of the polypeptide/dendron mixtures were considerably different from those corresponding to the individual polypeptides in terms of the significant reduction of intensity, discrete structure, and dislocation of characteristic bands. CD spectra deconvolution indicated that such spectral features resulted from the presence of a complex mixture, involving not only those typical for well-ordered proteins but also varying in the amount of distorted α-helix, and right- and left-hand twisted β-sheet, and sometimes the alternating presence of β-turns and β-sheets. The electrostatic attraction and multiple hydrogen bonding between oppositely charged molecules, that is, cationic branched peptides and the β-sheet surface formed by aggregating PLGA, were probably the main cause of co-aggregation that increased the variety and contribution of less ordered forms.

CONFLICT OF INTEREST

The authors declare no conflict of interest.

ORCID

Zofia Urbanczyk-Lipkowska https://orcid.org/0000-0003-2043-487X

REFERENCES

[1] P. Alam, K. Siddiqi, S. K. Chturvedi, R. H. Khan, *Int. J. Biol. Macromol.* **2017**, *103*, 208.
[2] R. A. M. Meijering, R. H. Henning, B. J. J. M. Brundel, *Trends Cardiovasc. Med.* **2015**, *25*, 243.
[3] B. Mannini, F. Chiti, *Front. Mol. Neurosci.* **2017**, *1*, 98.
[4] Y. L. Xiao, B. Y. Ma, D. McElheny, S. Parthasarathy, F. Long, M. Hoshi, R. Nussinov, Y. Ishii, *Nat. Struct. Mol. Biol.* **2015**, *6*, 499.
[5] C. K. Bett, W. K. Serem, K. R. Fontenot, R. P. Hammer, J. C. Garno, *ACS Chem. Neurosci.* **2010**, *1*, 661.
[6] C. Chunye, *Oxidative Med. Cell. Longev.* **2016**, *1*, 3571614.
[7] H. E. Lee, D. H. Kim, S. J. Park, J. M. Kim, Y. W. Lee, J. M. Jung, C. H. Lee, J. G. Hong, X. Liu, M. Cai, K. J. Park, D. S. Jang, J. H. Ryua, *Pharmacol. Biochem. Behav.* **2012**, *103*, 260.
[8] F. Karakida, Y. Ikeya, M. Tsunakawa, T. Yamaguchi, Y. Ikarashi, S. Takeda, M. Aburada, *Biol. Pharm. Bull.* **2007**, *30*, 514.
[9] E. Boschetti, P. G. Righetti, *J. Proteome* **2008**, *71*, 255.
[10] T. K. Lind, P. Zielinska, H. P. Wacklin, Z. Urbanczyk-Lipkowska, M. Cardenas, *ACS Nano* **2014**, *8*, 396.
[11] T. K. Lind, P. Polcyn, P. Zielinska, M. Cardenas, Z. Urbanczyk-Lipkowska, *Molecules* **2015**, *20*, 738.
[12] B. Klajnert, M. Cortijo-Arellano, J. Cladera, M. Bryszewska, *Biochem. Biophys. Res. Commun.* **2006**, *345*, 21.
[13] I. M. Neelov, A. Janaszewska, B. Klajnert, M. Bryszewska, N. Z. Makova, D. Hicks, H. A. Pearson, G. P. Vlasov, M. Y. Ilyash, D. S. Vasilev, N. M. Dubrovskaya, N. L. Tumanova, I. A. Zhuravin, A. J. N. N. Nalivaeva, *Curr. Med. Chem.* **2013**, *20*, 134.
[14] M. A. Dobrovolskaia, A. K. Patri, J. Simak, J. B. Hall, J. Semberova, S. H. D. P. Lacerda, S. E. McNeil, *Mol. Pharm.* **2012**, *9*, 382.
[15] E. L. Guzman, J. Amalraj, E. Fuentes, M. Alarcon, I. Palomo, I. Palomo, L. S. Santos, *Eur. J. Med. Chem.* **2013**, *69*, 601.
[16] H. Lee, J. H. Jeong, T. G. Park, *J. Control. Release* **2002**, *79*, 283.
[17] Y. Zhao, M. J. Haney, N. L. Klyachko, S. Li, S. L. Booth, S. M. Higginbotham, J. Jones, M. C. Zimmerman, R. L. Mosley, A. V. Kabanov, H. E. Gendelman, E. V. Batrakova, *Nanomedicine* **2010**, *6*, 25.
[18] R. H. Walters, R. M. Murphy, *J. Mol. Biol.* **2009**, *393*, 978.
[19] G. Bocchinfuso, P. Conflitti, S. Raniolo, M. Caruso, C. Mazzuca, E. Gatto, E. Placidi, F. Formaggio, C. Toniolo, M. Venanzi, A. Palleschi, *J. Pept. Sci.* **2014**, *20*, 494.
[20] A. Hernik, W. Puławski, B. Fedorczyk, D. Tymecka, A. Misicka, S. Filipek, W. Dzwolak, *Langmuir* **2015**, *31*, 10500.
[21] A. Hernik-Magoń, W. Puławski, B. Fedorczyk, D. Tymecka, A. Misicka, P. Szymczak, W. Dzwolak, *Biomacromolecules* **2016**, *17*(4), 1376.
[22] A. Micsonai, F. Wien, É. Bulyáki, Y.-H. Lee, Y. Goto, M. Réfrégiers, J. Kardos, *Nucleic Acids Res.* **2018**, *46*, W315.
[23] J. J. Grigsby, H. W. Blanch, J. M. Prausnitz, *Biophys. Chem.* **2002**, *99*, 107.
[24] M. Chittchang, H. H. Alur, A. K. Mitra, T. P. Johnston, *J. Pharm. Pharmacol.* **2002**, *54*, 315.
[25] N. Yamamoto, O. Kambara, K. Yamamoto, A. Tamura, S. Saito, K. Tominaga, *Soft Matter* **2012**, *8*, 1997.
[26] S. Song, S. A. Asher, *J. Am. Chem. Soc.* **1989**, *1989*(111), 4295.
[27] R. A. Hule, D. J. Pochan, *J. Polym. Sci. B Polym. Phys.* **2007**, *45*, 252.
[28] L. Mendonça, F. Hache, *Int. J. Mol. Sci.* **2012**, *13*, 2239.
[29] J. J. Balbach, A. T. Petkova, N. A. Oyler, O. N. Antzutkin, D. J. Gordon, S. C. Meredith, R. Tycko, *Biophys. J.* **2002**, *83*, 1205.
[30] S. Chimon, M. A. Shaibat, C. R. Jones, D. C. Calero, Y. Ishii, *PNAS* **1998**, *95*, 13407.
[31] M. C. Owen, D. Gnutt, M. M. Gao, S. K. T. S. Warmlander, J. Jarvet, A. Graslund, R. Winter, S. Ebbinghaus, S. B. Strodel, *Chem. Soc. Rev.* **2019**, *48*, 3946.
[32] *Nat. Protoc.* **2006**, *1*, 2876.

[33] H. Yao, E. Wynendaele, X. Xu, A. Kosgei, B. De Spiegeleer, *J. Pharm. Biomed. Anal.* **2018**, *147*, 50.
[34] A. Perczel, M. Hollosi, G. Tusnady, G. D. Fasman, *Protein Eng.* **1991**, *4*, 669.
[35] A. Micsonai, F. Wien, L. Kernya, Y.-H. Lee, Y. Goto, M. Réfrégiers, J. Kardos, *PNAS* **2015**, *112*, E3095.
[36] M. Michaelis, N. Hildebrand, R. H. Meißner, N. Wurzler, Z. Li, J. D. Hirst, A. Micsonai, J. Kardos, M. D. Piane, L. C. Ciacchi, *J. Phys. Chem. B* **2019**, *123*, 6694.
[37] B. Klajnert, J. Cladera, M. Bryszewska, *Biomacromolecules* **2006**, *7*, 2186.
[38] D. I. Andersson, D. Hughes, J. Z. Kubicek-Sutherland, *Drug Resist. Updat.* **2016**, *26*, 43.

SUPPORTING INFORMATION

Additional supporting information may be found online in the Supporting Information section at the end of this article.

How to cite this article: Morawiak M, Stolarska M, Cieślak M, Urbanczyk-Lipkowska Z. Interactions of rationally designed small peptide dendrons functionalized with valine or sinapic acid with α-helix and β-sheet structures of poly-L-lysine and poly-L-glutamic acid. *Pept Sci*. 2020;e24155. https://doi.org/10.1002/pep2.24155